

# A Machine Learning-based Approach for The Prediction of Electricity Consumption

Dinh Hoa Nguyen<sup>1</sup> and Anh Tung Nguyen<sup>2</sup>

**Abstract**—Balancing the power supply and demand is one of the most fundamental and important problems for the operation and control of any electric power grid. There are multiple ways to guarantee the supply-demand balance, but in this research we focus on one specific method to facilitate it namely the prediction of electricity consumption, which is widely used by utility companies or system operators. It is known that this prediction is challenging because of many reasons, for example, inexact weather forecasts, uncertain consumers' behaviors, etc. Hence, analytical and linear models of electricity consumption might not be able to deal with such issues well. This paper therefore presents a machine learning-based approach to predict electricity consumption, in which an improved radial basis function neural network (iRBF-NN) is proposed, whose inputs are time sampling points, temperature, and humidity associated with the consumption. The parameters of this iRBF-NN are sought by solving an optimization problem where four types of cost functions are used and compared on their performances and computational costs. Afterward, the derived model is employed to predict the future electricity consumption based on the hourly forecasts of temperature and humidity. Finally, simulation results for realistic data in Tokyo are presented to illustrate the efficiency of the proposed approach.

## I. INTRODUCTION

Energy plays an important role in many aspects of our daily lives where most of devices use electricity to operate and assist us to complete our works and enjoy our lives better. The lack of electricity causes severe problems to the society and economy, especially in peak hours. Hence, the prediction of electricity demand is an essential problem which is not only necessary for power utility companies but also for smart homes to schedule the power generation and consumption. For big cities with extremely large population such as Tokyo, electricity demand is huge. This will, undoubtedly, makes the problems of demand prediction and power scheduling more crucial. Additionally, new players in the electricity markets including renewable energy sources and distributed generation such as electric vehicles, energy storage systems, leads to new challenges for electricity demand prediction. All of the factors mentioned above contribute to the increasing interest on electricity demand forecast in recent years.

Basically, electricity consumption can be classified into two major types namely short-term (hourly, three hourly, one day, few days, and a week) and long-term (monthly,

and yearly) in [1]. The former is able to support the electricity manufacturer to plan for electricity generation and distribution appropriately. The latter is used to calculate the material input such as water, coal, and nuclear, for generators, or to install photovoltaic cell and wind turbine in case of renewable energy. In this research, we focus on the former type of electricity demand prediction, i.e., short-term prediction.

To predict the electric consumption, historical data on the past consumption, temperature, humidity, gross domestic product (GDP), population, types of households and their correlation coefficients, and user behaviors are often utilized. The behavior projection is known to use the data of people's habits in using electrical devices (which is not related with the environmental conditions and the weather) for prediction [2]. In contrast, the physical prediction is related with the weather and environmental conditions such as the season, amount of rain, temperature, humidity, and solar radiation. The work [3] applied ZABES (Zone Air Building Energy Simulation), which includes a building envelope model, external loads, and internal loads, to calculate building energy demand by solving the energy and mass balance equations of the zone air. In [4], a grey model was considered to describe and analyze the energy consumption in buildings with incomplete or uncertain data. The electricity consumption in buildings is also investigated by Artificial Neural Networks (ANNs) because there is a difference in patterns between buildings [5].

The study in [6] investigated the monthly average temperature and monthly electric consumption from April 2013 to September 2014 in 1100 households in Japan, and applied the Fourier transform (time series) to predict the future electricity consumption. Another time series method called the Gaussian process was also applied to predict the future electricity consumption. Two methods should be used to forecast the aggregated consumption based on the collected consumption in both short and long periods because individuals tend to use electricity unstably. Moreover, these methods are able to characterize data based on time and magnitude to make similar groups. The Gaussian process can indicate clearly changes in small intervals while the Fourier transform causes a large error. The authors in [7] used the support vector regression and fuzzy based on PSO algorithm to predict the short-term demand in South Korea. ANN was employed to predict both the aggregated and individual electricity consumption in [8] because this method can analyze highly nonlinear systems. However, the input-output relationship was not shown clearly to obtain groups from given data.

<sup>1</sup>Corresponding author. International Institute for Carbon-Neutral Energy Research (WPI-I2CNER), and Institute of Mathematics for Industry (IMI), Kyushu University, Fukuoka, Japan. Email: [hoa.nd@i2cner.kyushu-u.ac.jp](mailto:hoa.nd@i2cner.kyushu-u.ac.jp)

<sup>2</sup>Hanoi University of Science and Technology, Hanoi, Vietnam. Email: [tung.na134410@sis.hust.edu.vn](mailto:tung.na134410@sis.hust.edu.vn)

Although fuzzy logic can illustrate the relationship between input and output, this method also cannot separate historical data into small groups. Both approaches need a large number of data to train their networks to adjust parameters and cannot extrapolate the future electricity consumption. The research in [9] used a two-layer perceptron neural network to predict the electricity consumption with six inputs including the population, GDP per capita, inflation percentage, unemployment percentage, and winter/summer average temperature. To improve the accuracy of this method, the author also forecasts the future population. The authors in [10] proposed an electricity consumption regression model based on the linear combination of the GDP and the population or the GDP per capita.

It is also worth noting that most of the existing works only consider the temperature to predict the electricity consumption, while ignoring the humidity. However, the humidity is in fact an important factor affecting to the electricity consumption because human comfort is dependent on both temperature and humidity. Several standards have been made upon the indoor comfort zones, e.g., that by the American Society of Heating, Refrigerating and Air-Conditioning Engineers (ASHRAE) [11]. These standards have been used and further investigated in many studies, e.g., [12], [13]. Several models and methods to control the thermal comfort, for instance, ANNs, autoregressive variants, fuzzy control, and hybrid models was reviewed in [14].

In this paper, we aim at proposing an approach for predicting the day-ahead and intra-day hourly electricity consumption. Temperature, humidity, and the vector of time indexes are used as three inputs to an improved radial basis function neural network (iRBF-NN) [15] to predict the future electricity demand. In addition, several different cost functions are investigated in this iRBF-NN. The reason to use iRBF-NN is that the relationship between the electricity consumption and weather conditions including temperature and humidity is nonlinear, therefore linear models may not accurately predict the future consumption. We then introduce a method to derive a prediction interval or envelope with the percentage of prediction. In reality, this prediction interval is important because the electricity consumption is uncertain and one cannot exactly predict the future consumption.

The following notations and symbols will be used in the paper. The notation  $x_{[i],j}$  denotes the variable  $x$  for the  $j$ -th input in the  $i$ -th layer of the iRBF-NN. Then  $X_{[i],j}(k)$  is the  $k$ -th element of a vector  $x_{[i],j}$ , and  $X(i,k)$  denotes the  $(i,k)$ -th element of a matrix  $X$ . Next,  $\mathbb{R}$  stands for the set of real numbers, while  $\mathbf{1}_n$  is used for the vector having  $n$  elements equal to one. Last,  $|\bullet|$  stands for the absolute operator.

## II. MODEL DESCRIPTION OF iRBF-NN

In this section, we first explain why temperature and humidity are chosen as two of three inputs in our model. Table I shows the correlation of distinct weather parameters to the electricity consumption using the past data on realistic consumption in Tokyo [16], [17], where the closer to 1 the absolute value of the correlation is, the more related

to the electricity consumption the associated parameter will be. It can be seen that temperature and humidity have the highest correlation to the electricity consumption. Note that the sunshine duration has a reasonably high relative score but its data are usually hard to collect. Also, other factors like population, average consumption, etc., could affect to the electric consumption, however we do not consider here for simplicity of the model.

TABLE I  
CORRELATION BETWEEN WEATHER PARAMETERS AND ELECTRIC CONSUMPTION FROM 25/9/2018 TO 25/10/2018 IN TOKYO.

Parameters	Correlation value
temperature	0.53
relative humidity	-0.43
precipitation	0.1
sunshine duration	0.37
wind speed	0.2

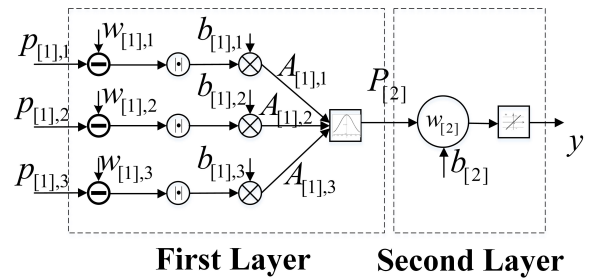


Fig. 1. Description of the iRBF-NN.

Next, the iRBF-NN model used in this research is presented, which composes of two layers. The first layer composes of  $m$  neurons whose outputs are fed to a nonlinear Gaussian function while the second layer is a pure linear function with bias.

The input vector to the iRBF-NN includes  $p_{[1],1}, p_{[1],2}$ , and  $p_{[1],3}$ , in which  $p_{[1],1}$  is the vector of time indexes (hours),  $p_{[1],2}$  is the historical temperature ( $^{\circ}\text{C}$ ), and  $p_{[1],3}$  is the historical humidity (%). The dimensions of the variables are as follows. The inputs  $p_{[1],j} \in \mathbb{R}^N$  for  $j = 1, 2, 3$ , and the output matrix of the first layer  $A_{[1],j} \in \mathbb{R}^{m \times N}$ , where  $N$  is the number of hours at which the historical data is collected.  $w_{[1],j} \in \mathbb{R}^m$  and  $b_{[1],j} \in \mathbb{R}^m$  are the weight and bias vector; respectively. Consequently,  $P_{[2]} \in \mathbb{R}^{3m \times N}$  is the input matrix to the second layer. The output vector and the target vector of historical electricity consumption are denoted by  $y \in \mathbb{R}^N$  [10 MWh] and  $t \in \mathbb{R}^N$  [10 MWh]. Finally,  $w_{[2]} \in \mathbb{R}^{3m}$  and  $b_{[2]} \in \mathbb{R}$  are the weight vector and the bias in the second layer.

$$A_{[1],j}(i,k) = |p_{[1],j}(k) - w_{[1],j}(i)| b_{[1],j}(i) \quad (1)$$

$$A_{[1]} = [A_{[1],1}^T, A_{[1],2}^T, A_{[1],3}^T]^T \quad (2)$$

$$P_{[2]} = \text{radbas}(A_{[1]}) \quad (3)$$

$$y = P_{[2]}^T w_{[2]} + b_{[2]} \mathbf{1}_N \quad (4)$$

Using this model and the historical data on electricity consumption, temperature, and humidity, the model parameters are trained so that  $y \rightarrow t$ , i.e., the estimated model for the existing data is derived. Finally, the obtained model parameters in the estimated model are used to predict the future electricity consumption based on the forecast of hourly temperature and hourly humidity.

### III. DATA FITTING METHODS

Originally, the iRBF-NN utilizes the  $L_2$  cost function, i.e., the least-square method to find the model parameters to fit the model output  $y$  to the existing data  $t$ . However, in this research we attempt to employ several different cost functions to verify their effectiveness on the prediction accuracy. Particularly, the following cost functions are considered:

$$J_1 = \sum_{k=1}^N |y(k) - t(k)| \quad (5)$$

$$J_2 = \sum_{k=1}^N [y(k) - t(k)]^2 = (y - t)^T (y - t) \quad (6)$$

$$J_3 = \sum_{k=1}^N \left\{ [y(k) - t(k)]^2 + \beta |y(k) - t(k)| \right\} \quad (7)$$

Hereafter, we denote the cost functions (5), (6), and (7) by  $L_1$ ,  $L_2$ , and  $L_1 \& L_2$ ; respectively. The parameter  $\beta$  can be selected to compromise between the performance and the computational cost. Denote

$$x \triangleq \begin{bmatrix} w_{[2]} \\ b_{[2]} \end{bmatrix}, \quad U \triangleq \begin{bmatrix} P_{[2]} \\ \mathbf{1}_N^T \end{bmatrix} \quad (8)$$

Then (6) can be rewritten as

$$J_2 = (U^T x - t)^T (U^T x - t) \quad (9)$$

of which the optimal solution is

$$x^* = (UU^T + \rho I)^{-1} U t \quad (10)$$

The small term  $\rho > 0$  is added to (10) because  $UU^T$  may not be invertible. This optimal solution gives us all parameters of the second layer while the parameters of the first layer in the iRBF-NN are fixed *a priori*.

The  $L_1$  cost function (5) is also studied here because it is known to be more robust to outliers than the  $L_2$  cost function [18, Chapter 6], which is important to the estimation and prediction problems because of the possible inaccuracies on the temperature and humidity forecast. In order to find the optimal solutions of (5) and (7), one method is to utilize the optimal solution of (10) to solve them iteratively. To do so, rewrite (5) as follows,

$$J_1 = \sum_{k=1}^N \frac{1}{|y(k) - t(k)|} [y(k) - t(k)]^2 \quad (11)$$

At the  $l$ -th iteration ( $l > 1$ ), we set

$$J_1(l) = \sum_{k=1}^N \frac{1}{|y_l(k) - t(k)|} [y_l(k) - t(k)]^2 \quad (12)$$

where  $y_l(k)$  is  $k$ -th element of vector  $y$  at the  $l$ -th iteration. Given a tolerance  $\varepsilon > 0$ , this iterative algorithm is stopped, i.e.,  $y_l \rightarrow y^* \triangleq \arg \min J_1$ , if

$$\|y_l - y_{l-1}\|_2 \leq \varepsilon \quad (13)$$

Next, (12) can be approximated as follows,

$$J_1(l) = \sum_{k=1}^N \frac{1}{|\theta_{l-1}(k) - t(k)|} [y_l(k) - t(k)]^2 \quad (14)$$

where  $\theta_l = \mathbf{1}_N$  and  $l$  runs from 2. The parameter  $\theta_{l-1}(k)$  in (14) can be  $y_{l-1}(k)$  or the average of  $y_{l-1}(k)$ ,  $y_{l-2}(k), \dots, y_2(k)$ . We call the latter choice the  $L_1^*$  cost function. Denote

$$\alpha_l(k) \triangleq \frac{1}{|\theta_{l-1}(k) - t(k)|}, \quad \Lambda_l \triangleq \text{diag}(\alpha_l(1), \alpha_l(2), \dots, \alpha_l(N)) \quad (15)$$

Substituting  $\alpha_l(k)$  and  $\Lambda_l$  into (14) gives us

$$J_1(l) = (y_l - t)^T \Lambda_l (y_l - t) \quad (16)$$

The optimal solution of (16), similar to (10), is

$$x_l^* = (U \Lambda_l U^T + \rho I)^{-1} U \Lambda_l t \quad (17)$$

On the other hand, if the  $L_1 \& L_2$  cost function (7) is used to estimate the iRBF-NN parameters, then the optimal solution can be derived in a similar manner as above to be

$$x_l^* = [U(I + \beta \Lambda_l)U^T + \rho I]^{-1} U(I + \beta \Lambda_l)t \quad (18)$$

Subsequently, the following steps are presented to summarize the iterative process for solving the  $L_1$ ,  $L_1^*$ , and  $L_1 \& L_2$  methods.

- Step 1: Set  $l = 1$  and select the tolerance  $\varepsilon$ . Then set  $y_l = \mathbf{1}_N$ .
- Step 2: Set  $l = l + 1$ . Calculate  $\Lambda_l$  from (15) and find  $x_l^*$  from (17) or (18).
- Step 3: Find vector  $w_{[2]}$  and  $b_{[2]}$  from (8).
- Step 4: Compute  $\theta_l$ .
- Step 5: Examine (13). If true, going to step 6, otherwise go back to step 2.
- Step 6: Obtain the optimal solution  $y_l(k)$ .

After the parameters of the second layer is found, the predicted consumption  $y_{pre}$  can be obtained by putting the prediction input  $p_{pre}$ . The Mean Absolute Percentage Error (MAPE) coefficient (19) is selected to evaluate the error between the real data and the estimated value or the predicted value.

$$MAPE = \frac{100\%}{N} \sum_{k=1}^N \left| \frac{t(k) - y(k)}{t(k)} \right| \quad (19)$$

Next, because the weather forecast including that for temperature and humidity is not precise and there are uncertainties on end-user behaviors, the prediction of electricity consumption in reality is often required in form of a prediction interval. Therefore, we introduce in the following two methods to generate an envelope of the predicted electricity consumption for a given probability of exactness. In the first

method, the upper bound and lower bound of this envelope can be calculated as follows:

$$y_{up} = y_{pre} + z^\alpha \sigma \quad (20)$$

$$y_{low} = y_{pre} - z^\alpha \sigma \quad (21)$$

where  $z^\alpha$  and  $\sigma$  are 100 $\alpha$  percentile of a normal deviation and the standard deviation of the past electricity consumption; respectively, for example  $z^{0.8} = 1.282$ . During working days, usually the electricity consumption largely varies where the consumed energy in the late evening and early morning (from 10 pm to 7 am) is far less than that in the other hours. Therefore, the standard deviation  $\sigma$  can be calculated to generate the envelope of the prediction interval at each hour in a day.

In the second method, the envelope of the predicted electricity consumption is generated by the well-known bootstrap method [19]. A fixed number of days in the historical data will be randomly picked up to derive the parameters of the iRBF-NN model, and then the obtained model will be utilized to predict the electricity demand in the future. This process is repeated many times to generate the set of predicted demand curves, i.e., an estimation of the prediction interval. Afterward, the mean of those demand curves is set to be the predicted electricity demand, while the maximum and minimum of 90% of this set will create the boundaries of the predicted envelope for the electricity demand.

#### IV. TEST CASES

The historical temperature, humidity and hourly electricity consumption data in Tokyo are collected on working days during the period between 25 September and 25 October 2018 [16], [17]. Because of the limited data, the number of neurons is selected to be  $m = 100$ . Lastly,  $\rho = 10^{-4}$ ,  $\varepsilon = 0.1$ .

The parameters of the second layer in the RBF-ANN is found by minimizing the cost functions (5), (6), and (7) with collected data of weather and electricity consumption. Consequently, the electricity on 26 October 2018 will be predicted based on the day-ahead weather forecast, i.e., on 25 October, and the intra-day weather forecast at 0 am of 26 October. The day-ahead prediction is useful for the power scheduling of utility companies, while the intra-day forecast is useful to adjust the power scheduling better.

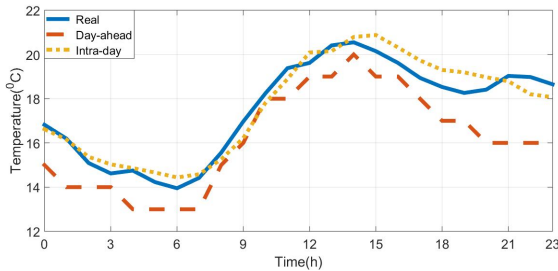


Fig. 2. Temperature in Tokyo on 26 October 2018.

Figures 2–3 display the realistic weather data, and their day-ahead and intra-day forecasts used in the simulations.

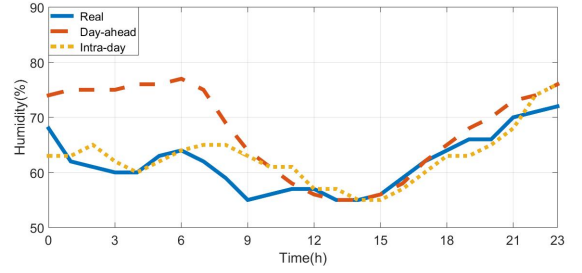


Fig. 3. Humidity in Tokyo on 26 October 2018.

We can easily observe that the accuracy of the temperature and humidity forecasts are low.

#### A. Performance Comparison of Four Cost Functions

The comparisons for estimation and prediction using four cost functions are shown in Table II and are visualized in Figure 4. It can be seen that there are no big differences on the estimation errors of different cost functions, but the prediction errors of the  $L_1$  and  $L_1^*$  cost functions are smaller than that of the others. This is understandable because the  $L_1$  programming is known to be more robust to outliers, in this case is the impreciseness of the weather forecasts, than the  $L_2$  programming. Nevertheless, there is a trade-off between the performance and the computation cost since the  $L_1$  and  $L_1^*$  cost functions induce much longer computational times.

TABLE II

PERFORMANCE COMPARISON AMONG FOUR TYPES OF COST FUNCTIONS

Cost Function	MAPE (%)			Estimation time (second)
	Estimation	Day ahead Prediction	Intra-day Prediction	
$L_2$	1.7121	1.9748	1.8315	3
$L_1$	1.5907	1.4739	1.6824	489
$L_1 \& L_2$	1.6651	2.0676	1.8712	64
$L_1^*$	1.6000	1.4324	1.6903	650

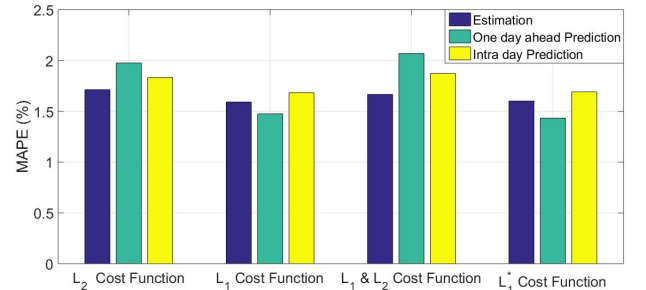


Fig. 4. The comparison among four types of cost functions

#### B. Day-ahead vs. Intra-day Prediction

Both the day-ahead and the intra-day predictions for the electricity consumption on 26 October 2018 using four types of cost functions are displayed in Figures 5–8. It can be seen that for all types of cost functions, there are gaps between

the day-ahead as well as the intra-day prediction and the real electricity consumption, especially in the early morning. This can be explained by the large forecasting errors on the temperature and humidity at that time period.

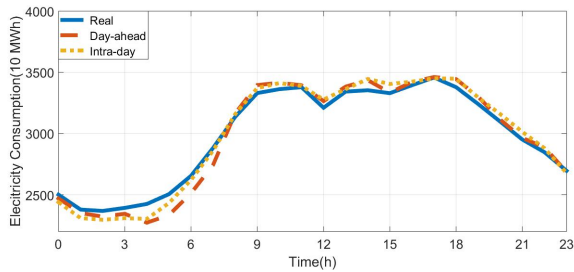


Fig. 5. Day-ahead and intra-day prediction with  $L_2$  cost function.

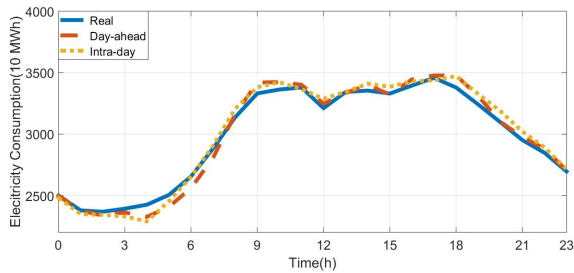


Fig. 6. Day-ahead and intra-day prediction with  $L_1$  cost function.

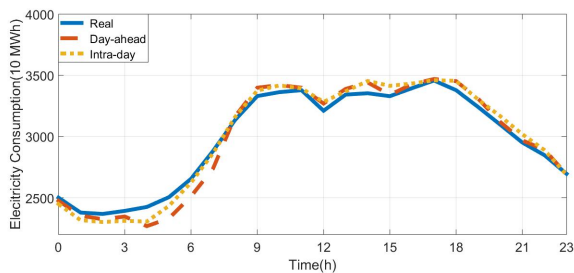


Fig. 7. Day-ahead and intra-day prediction with  $L_1&L_2$  cost function.

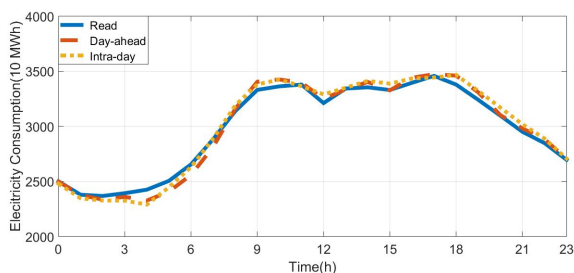


Fig. 8. Day-ahead and intra-day prediction with  $L_1^*$  cost function.

In addition, there are gaps between day-ahead and intra-day predictions due to the differences on the day-ahead and

intra-day weather forecasts, where the intra-day prediction is better in the early morning.

### C. Prediction Interval

The prediction interval using the first method and four types of cost functions are exhibited in Figures 9–12, in which  $\alpha = 0.8$ . The computational time of this method is fast, however the prediction interval is large, especially during the peak time period.

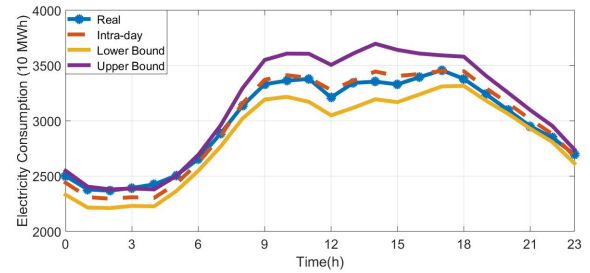


Fig. 9. Intra-day prediction interval with  $L_2$  cost function by the first method.

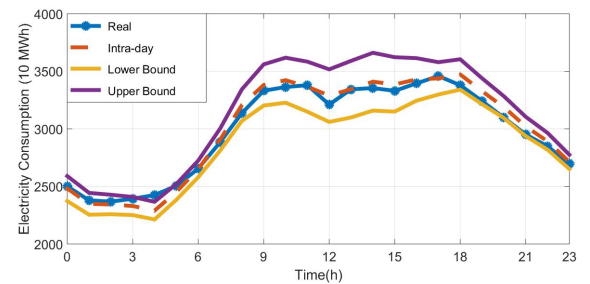


Fig. 10. Intra-day prediction interval with  $L_1$  cost function by the first method.

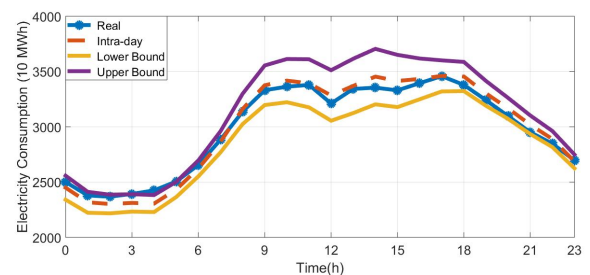


Fig. 11. Intra-day prediction interval with  $L_1&L_2$  cost function by the first method.

For the bootstrap method, 16 days are chosen randomly from 22 days of data to find the parameters of the iRBF-NN in 1000 estimations, which then are used to generate 1000 predictions in Figure 13. Next, the maximum and minimum of 90% of those 1000 lines are used to get the prediction interval in Figure 14. The bootstrap-based method is more meaningful than the first method in term of prediction because it uses the many predictions to compute the boundaries

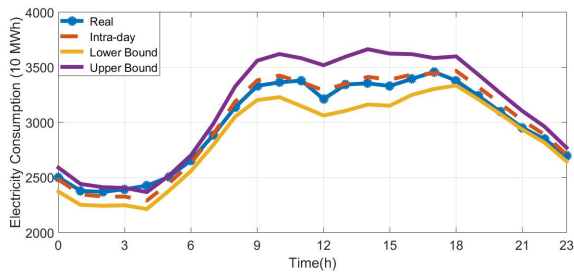


Fig. 12. Intra-day prediction interval with  $L_1^*$  cost function by the first method.

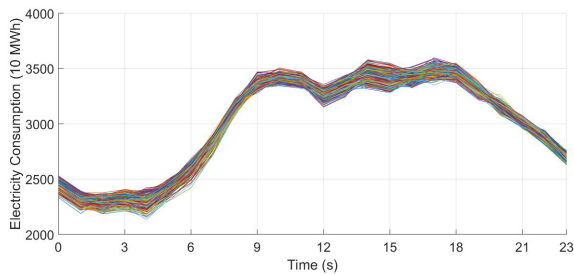


Fig. 13. One thousand of intra-day predictions with  $L_2$  cost function using the bootstrap method.

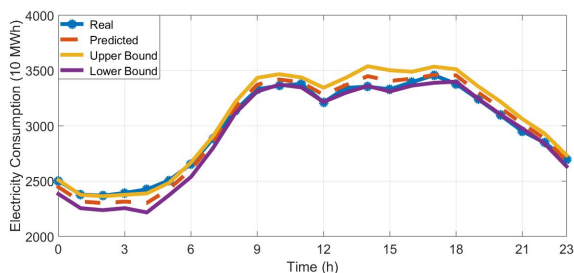


Fig. 14. Intra-day prediction interval with  $L_2$  cost function generated by the bootstrap method.

of the prediction interval whilst the first method employs the past data to create those boundaries. However, the bootstrap takes much more computational time.

## V. CONCLUSIONS

In this paper, a machine learning-based approach namely iRBF-NN is proposed for the prediction of electricity consumption using available Tokyo's realistic data on the consumption and the weather in the past and the weather forecast in the future. Unlike other existing approaches which use only the temperature, in our proposed approach several weather parameters can be used as the input data. After analyzing the correlation of such weather parameters to the historical electricity consumption, the hourly temperature and humidity are selected as two inputs to the iRBF-NN. Then four types of optimization cost functions are employed and compared on their estimation and prediction performance as well as their computational times. Additionally, the predic-

tion interval is also studied by two methods whose comparisons are obtained in the test cases. Overall, the estimation and prediction performances of the proposed approach are good for all types of optimization cost functions, in which the  $L_1$  cost function seems to be the best, even though the weather forecast is not precise.

## REFERENCES

- [1] H. S. Hippert, C. E. Pedreira, R. C. Souza, Neural Networks for Short-Term Load Forecasting: A Review and Evaluation, *IEEE Transactions on Power Systems*, vol. 16, pp. 44–55, 2001.
- [2] R. Yao, K. Steemers, A method of formulating energy load profile for domestic building in the UK, *Energy and Buildings*, vol. 37, pp. 663–671, 2005.
- [3] R. P. Kramer, A. W. M. van Schijndel, H. L. Schellen, The importance of integrally simulating the building, HVAC and control systems, and occupants impact for energy predictions of buildings including temperature and humidity control: validated case study museum Hermitage Amsterdam, *Journal of Building Performance Simulation*, vol. 10, pp. 272–293, 2017.
- [4] J. J. Guo, J. Y. Wu, R. Z. Wang, A new approach to energy consumption prediction of domestic heat pump water heater based on grey system theory, *Energy and Buildings*, vol. 43, pp. 1273–1279, 2011.
- [5] K. Li, C. Hu, G. Liu, W. Xue, Building's electricity consumption prediction using optimized artificial neural networks and principal component analysis, *Energy and Buildings*, vol. 108, pp. 106–113, 2015.
- [6] A. Ozawa, R. Furusato, Y. Yoshida, Determining the relationship between a households lifestyle and its electricity consumption in Japan by analyzing measured electric load profiles, *Energy and Building*, vol. 119, pp. 200–210, 2016.
- [7] H. Son, C. Kim, Short-term forecasting of electricity demand for the residential sector using weather and social variables, *Resources, Conservation and Recycling*, vol. 123, pp. 200–207, 2017.
- [8] F. McLoughlin, A. Duffy, M. Conlon, Evaluation of time series techniques to characterise domestic electricity demand, *Energy*, vol. 50, pp. 120–130, 2013.
- [9] M. E. Gunay, Forecasting annual gross electricity demand by artificial neural networks using predicted values of socio-economic indicators and climatic conditions: Case of Turkey, *Energy Policy*, vol. 90, pp. 92–101, 2016.
- [10] V. Bianco, O. Manca, S. Nardini, Linear Regression Models to Forecast Electricity Consumption in Italy, *Energy Sources, Part B: Economics, Planning, and Policy*, vol. 8, pp. 86–93, 2013.
- [11] ASHRAE, Thermal environmental conditions for human occupancy. [Online]. Available at: <https://www.ashrae.org/technical-resources/bookstore/standard-55-thermal-environmental-conditions-for-human-occupancy>
- [12] C. C. Okaeme, S. Mishra, J. T. Wen, A Comfort Zone Set-Based Approach for Coupled Temperature and Humidity Control in Buildings, *IEEE International Conference on Automation Science and Engineering*, USA, 2016, pp. 456–461.
- [13] F. R. A. Alfano, B. W. Olesen, B. I. Palella, G. Riccio, Thermal comfort: Design and assessment for energy saving, *Energy and Buildings*, vol. 81, pp. 326–336, 2014.
- [14] D. Enescu, A review of thermal comfort models and indicators for indoor environments, *Renewable and Sustainable Energy Reviews*, vol. 79, pp. 1353–1379, 2017.
- [15] M. T. Hagan, H. B. Demuth, M. H. Beale, O. D. Jesus, *Neural Network Design*, 2nd Edition, New York, USA, 2014.
- [16] <https://www.timeanddate.com/weather/japan/tokyo/hourly>
- [17] <http://www.tepco.co.jp/en/forecast/html/download-e.html>
- [18] S. Boyd, N. Parikh, E. Chu, B. Peleato, and J. Eckstein, Distributed Optimization and Statistical Learning via the Alternating Direction Method of Multipliers, *Foundations and Trends in Machine Learning*, vol. 3, pp. 1–122, 2011.
- [19] M. Joshi, A. S. Morgenstern, A. Kremling, Exploiting the bootstrap method for quantifying parameter confidence intervals in dynamical systems, *Metabolic Engineering*, vol. 8, pp. 447–455, 2006.